Proceedings of the 2008 IEEE
International Conference on Information and Automation
June 20 -23, 2008, Zhangjiajie, China

Energy Harvesting and Dissipation with Piezoelectric Materials

Junrui Liang and Wei-Hsin Liao
Smart Materials and Structures Laboratory
Department of Mechanical and Automation Engineering
The Chinese University of Hong Kong
Shatin, N. T., Hong Kong, China
E-mails: jrliang@mae.cuhk.edu.hk, whliao@mae.cuhk.edu.hk

***Abstract*— This paper proposes a comparative analysis to clarify the functions of piezoelectric energy harvesting, dissipation and their effects on structural damping. Energy flow in piezoelectric devices is discussed. Based on the equivalent circuit, the damping effects resulted from energy harvesting in the application of standard energy harvesting and energy dissipation in the application of resistive shunt damping are investigated. Comparison between these two applications is made, in terms of loss factor. Experiments based on the same base-driven piezoelectric cantilever are carried out to verify the theoretical analysis. It is shown that experimental data match the analytical results very well.**

I. Introduction

Over the past few years, with the pursuit of reliable power solutions to extend the lifespan and territory of portable and wireless electronics or microsystems, the techniques of energy harvesting have been put under spotlight. One of the promising sources, from which people would like to collect energy, is mechanical vibration. Three transduction mechanisms (i.e. piezoelectric, electromagnetic, and electrostatic) were studied in order to reclaim the ambient vibration energy and turn it into useful electrical power. Among generators based on these three mechanisms, the piezoelectric ones are the simplest to fabricate [1], therefore, they are particularly suitable for implementation in microsystems.

Up to now, most of the researches on piezoelectric energy harvesting were mainly concerned with the absolute energy that can be harvested from vibrating structure [2]–[4]. The effect, which is resulted from energy harvesting and reacts to the vibrating structure, was seldom discussed in these studies. Lesieutre et al. discussed such an issue and claimed that the harvesting of electrical energy from the piezoelectric system brings out structural damping [5]. On the other hand, it has been known for a long time that the effect of structural damping can be caused by energy dissipation. In most of the shunt damping treatments, energy dissipation was regarded as the only function that contributes to structural damping [6].

In this paper, the relationship among the functions of energy harvesting, dissipation and their effects on structural damping will be investigated. This understanding is crucial towards an adaptive energy harvesting technique. In section II, we give an explanation to the energy flow in piezoelectric devices. In section III, the functions of harvesting and dissipation are considered respectively in two individual piezoelectric applications. Following this, a comparison between these two applications is given, in terms of damping capability. To verify this theoretical analysis, experiments on these two applications, which are based on the same mechanical structure, are performed. Experimental results and discussions are provided in section IV. Finally, a conclusion is given in section V.

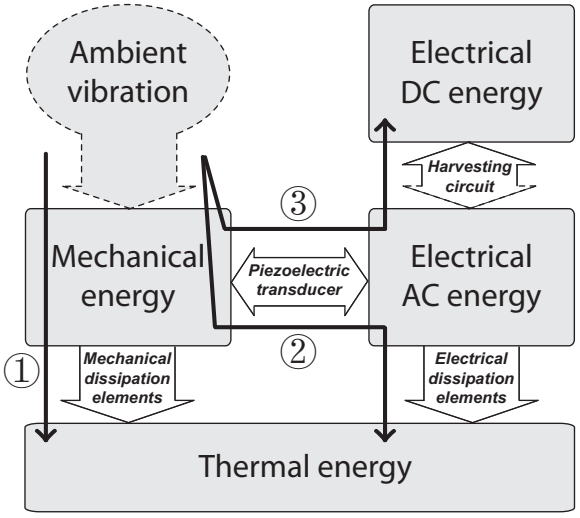

Fig. 1. Energy flow chart in piezoelectric devices.

II. Energy flow in piezoelectric devices

In most literature, damping is the dissipation of energy of a mechanical system [7], [8], and dissipation usually means the lost energy is converted into heat. However, it was also pointed out [8] that damping is the process that converts and dissipates mechanical energy into other forms of energy. Considering the piezoelectric energy harvesting, which also results in structural damping, the previous definition needs to be clarified.

Fig. 1 provides an overview on three forms of energy involved in the piezoelectric devices. These three forms are: mechanical, electrical, and thermal. The previous twos are linked by the bi-directional piezoelectric transducer. At the same time, either mechanical or electrical energy can be converted into thermal by dissipation elements such as mechanical dampers or electrical resistors. Once the energy is dissipated,

978-1-4244-2184-8/08/$25.00 © 2008 IEEE.

TABLE I

TERMS SPECIFICATION

Paths	Functions		Effect
①	Mechanical energy dissipation	Energy dissipation (dissipation factor)	Vibration damping (loss factor)
②	Electrical energy dissipation		
③	Energy harvesting (harvesting factor)		

i.e. transform into heat, it will not be recovered in these devices, therefore dissipative transformation is uni-directional. From the energy flow shown in Fig. 1, we can sort out three paths: path ① is *mechanical energy dissipation*; path ② is *electrical energy dissipation*; and path ③ is *energy harvesting*.

The three paths in Fig. 1 represents three *functions* that can remove energy from the piezoelectric system. One or more of these functions can take place in certain *applications* and cause the *effect* of structural damping. TABLE I gives the terms specification for the three functions that can remove mechanical energy from vibrating structures.

The three factors within the parentheses in TABLE I are indices to evaluate the corresponding functions or effect. For traditional damping, the term *loss factor* was usually used to evaluate the total damping capability. It was defined as the ratio between the energy dissipated per cycle and the maximum energy associated with vibration [9]. Here, in order to continue using this term for damping evaluation, we make a subtle change in this old definition. The new defined loss factor is the ratio between the energy removed per cycle and the maximum energy associated with vibration. Moreover, considering energy harvesting, it is not enough to show the detailed energy relations with the use of loss factor only. Therefore, two additional factors are defined with respect to energy harvesting and energy dissipation as follows.

For energy harvesting, the new term *harvesting factor* is defined to evaluate the harvesting capability as

$$\eta_h = \frac{E_h}{2\pi E_{max}}, \tag{1}$$

where E_h denotes the harvested energy in one cycle, E_{max} is the maximum energy associated with vibration, i.e. summation of both mechanical and electrical AC energy.

For energy dissipation, the term *dissipation factor* is used to evaluate the dissipation capability as

$$\eta_d = \frac{E_d}{2\pi E_{max}}, \tag{2}$$

where E_d is the dissipated energy in one cycle.

With Eq. (1) and Eq. (2), we can define the *loss factor* as

$$\eta_\Sigma = \frac{\Delta E}{2\pi E_{max}} = \eta_h + \eta_d, \tag{3}$$

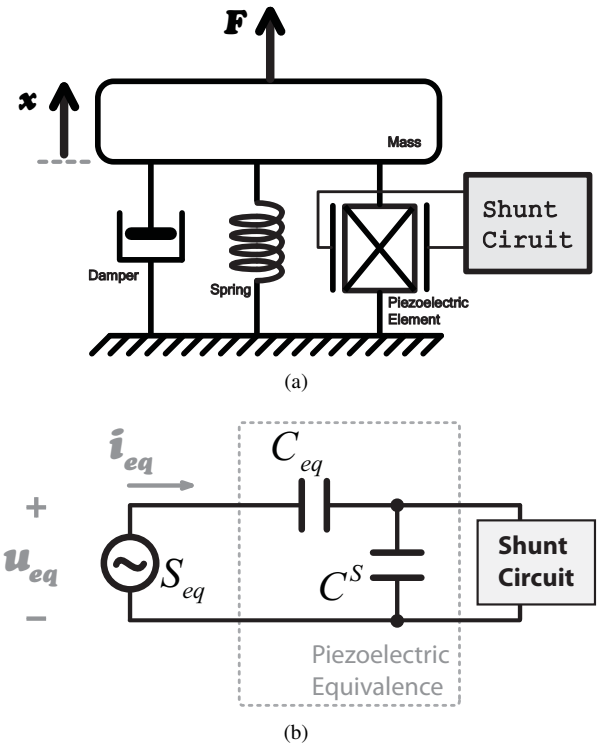

Fig. 2. Schematic representation and equivalent circuit of a piezoelectric device. (a) Schematic representation. (b) Equivalent circuit.

where ΔE is the summation of E_h and E_d, which represents the total removed energy from the vibrating structure in one cycle.

III. ENERGY HARVESTING AND DISSIPATION

A. Equivalent circuit

Taking single degree-of-freedom approximation, a piezoelectric device can be simply modeled as a second-order mass-spring-damper system as shown in Fig. 2(a). The dynamic behavior or this electro-mechanical model can be simulated by a equivalent circuit [9], which is given in Fig. 2(b). In the equivalent circuit, u_{eq} and i_{eq} are equivalent voltage and equivalent current associated with mechanical force F and velocity $\dot{x}$. Their relationships are given by

$$\begin{cases} u_{eq} = F/\alpha_e \\ i_{eq} = \dot{x}\alpha_e \end{cases}, \tag{4}$$

where α_e is the piezoelectric force-voltage coupling factor. It is related to the piezoelectric coupling coefficient k_m^2 with the relation as follows

$$k_m^2 = \frac{\alpha_e^2}{K^E C^S + \alpha_e^2}. \tag{5}$$

K^E and C^S are short circuit stiffness and clamped capacitance of the piezoelectric element, respectively.

C_{eq} in the circuit is the equivalent capacitance corresponding to the short circuit stiffness of the piezoelectric patch

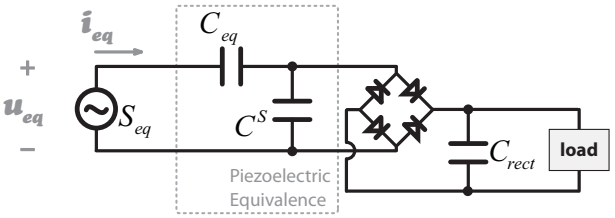

Fig. 3. Equivalent circuit for standard energy harvesting.

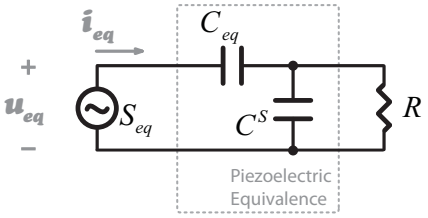

Fig. 4. Equivalent circuit for resistive shunt damping.

$$C_{eq} = \frac{\alpha_e^2}{K^E}. \tag{6}$$

Regardless of the purposes of energy harvesting or structural damping, the mechanical parts of their devices are similar in structure. Most of the differences lie in their shunt circuits. Therefore, this equivalent circuit can serve as a common base for both analyses of energy harvesting and dissipation.

B. Harvesting factor in standard energy harvesting

In the standard energy harvesting application, only the energy harvesting function contributes to the effect of structural damping. The shunt circuit is a nonlinear circuit, which is composed of a bridge rectifier, a filter capacitor, and other loads in parallel. Its equivalent circuit is shown in Fig. 3. In analyzing this circuit, the DC filter capacitor C_{rect} is assumed to be large enough so that the voltage across this capacitor V_{rect} is nearly constant [2].

The ratio between the harvested energy and maximum stored energy, which is called *harvesting factor* in this paper, is a function of material coupling coefficient and V_{rect} [9]

$$\eta_h = \frac{4}{\pi}\tilde{V}_{rect}\frac{1-\tilde{V}_{rect}}{\frac{1-k_m^2}{k_m^2}+\tilde{V}_{rect}}, \tag{7}$$

where $\tilde{V}_{rect}$ is obtained by non-dimensionalizing the rectified voltage to the amplitude of open circuit voltage, i.e.

$$\tilde{V}_{rect} = \frac{V_{rect}}{V_{oc}}. \tag{8}$$

The material coupling coefficient depends on material and geometry properties, which cannot be changed after the device is made. The maximum harvesting factor can be obtained as follows

$$\eta_{h,max} = \frac{4}{\pi}\frac{\left(1-\sqrt{1-k_m^2}\right)^2}{k_m^2}, \tag{9}$$

at a non-dimensional rectified voltage

$$\tilde{V}_{rect,opt} = \frac{1-k_m^2}{k_m^2}\left(\sqrt{\frac{1}{1-k_m^2}}-1\right). \tag{10}$$

The optimum rectified voltage can be achieved by properly choosing a load. This load can be an adaptive DC-DC converter [2] or optimal resistor [10]. The extracted power is transferred or consumed so as to keep the optimum rectified voltage constant.

C. Dissipation factor in resistive shunt damping

In the application of resistive shunt damping [11], only the energy dissipation function contributes to the effect of structural damping. The equivalent circuit is shown in Fig. 4. It only connects a resistor as its shunt circuit to dissipate the extracted energy, thus results in damping. The dissipation factor is given by

$$\eta_d = \frac{\rho\ k_m^2}{1-k_m^2+\rho^2}, \tag{11}$$

where ρ is the non-dimensional shunt resistance

$$\rho = RC^S\omega, \tag{12}$$

and ω is the excitation angular frequency. The maximum dissipation factor can be obtained as follows

$$\eta_{d,max} = \frac{k_m^2}{2\sqrt{1-k_m^2}}, \tag{13}$$

at a non-dimensional resistance of

$$\rho_{opt} = \sqrt{1-k_m^2}. \tag{14}$$

D. Comparison

To compare the characteristics between standard energy harvesting and resistive shunt damping, we employ the non-dimensional voltage-charge diagrams to illustrate their energy conversion cycles.

Since the equivalent current in Fig. 2(b) equals to $\dot{x}\alpha_e$, the equivalent charge input is the integral of this current, which is $x\alpha_e$. Assuming X as the maximum displacement, the maximum equivalent input charge should be $X\alpha_e$. Non-dimensionalizing $x\alpha_e$ with $X\alpha_e$, we have

$$\tilde{q}_{eq} = \frac{x\alpha_e}{X\alpha_e} = \frac{x}{X}. \tag{15}$$

Similarly, we can also non-dimensionalize the equivalent input voltage F/α_e with respect to the open circuit voltage V_{oc}. Since

$$V_{oc} = \frac{X\alpha_e}{C_m} = \frac{K^E X}{\alpha_e}, \tag{16}$$

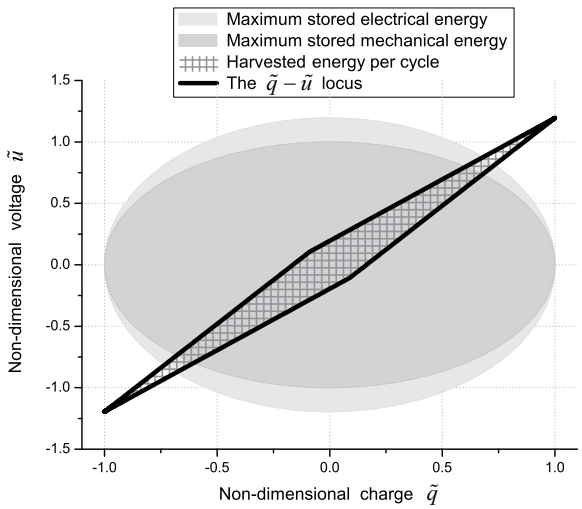

(a)

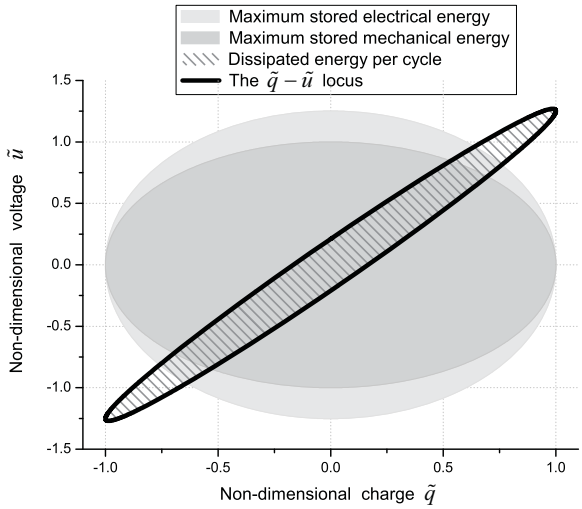

(b)

Fig. 5. Energy cycles in two applications. (a) Standard energy harvesting. (b) Resistive shunt damping.

we have

$$\tilde{u}_{eq} = \frac{F/\alpha_e}{V_{oc}} = \frac{F}{K^E X}. \tag{17}$$

Given the situation that $k_m^2 = 0.3$, for instance, the energy conversion cycles for standard energy harvesting with optimum V_{rect} and resistive shunt damping with optimum R are shown in Fig. 5(a) and (b), respectively. The black solid curve in either diagram shows the relation between non-dimensional charge and non-dimensional voltage in one cycle. The areas of gray ellipses represent 2π multiplying the maximum stored energy in the devices: lighter gray for electrical and darker one for mechanical. The areas enclosed by the $\tilde{q}-\tilde{u}$ loci represent the energy removed from the structures in one cycle. But in order to distinguish whether the extracted energy is harvested or dissipated, different patterns are used in the diagrams. With areas in different patterns representing energy in different forms, we can figure out the energy flow within these devices.

Without energy being dissipated, the maximum harvesting factor in standard energy harvesting is also the maximum loss factor; similarly, without energy being harvested, the maximum dissipation factor in resistive shunt damping is also the maximum loss factor. According to the relations given in Eq. (9) and Eq. (13), the two maximum loss factors, i.e. $(\eta_{\Sigma,max})_{SEH}$ and $(\eta_{\Sigma,max})_{RSD}$,[1] in the two applications, as functions of k_m^2, are compared in Fig. 6. As k_m^2 increases, the attainable maximum loss factors for both applications increase; besides, the ratio between the two factors of standard energy harvesting and resistive shunt damping decreases. Moreover, it should be noted that, when the material coupling coefficient approaches zero, we can obtain

$$\lim_{k_m^2 \to 0} \frac{(\eta_{\Sigma,max})_{SEH}}{(\eta_{\Sigma,max})_{RSD}} = \frac{2}{\pi} = 63.66\% \tag{18}$$

[1]The subscript SEH stands for standard energy harvesting; while RSD stands for resistive shunt damping.

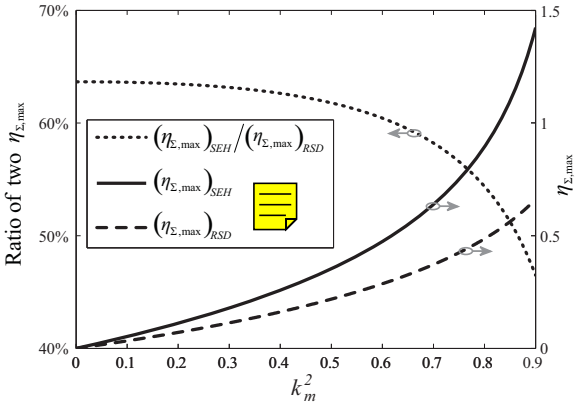

Fig. 6. Maximum loss factors in two applications and their ratio.

which can also be observed from the dot curve in Fig. 6. Lesieutre et al. had come up with the same result under this special condition [5].

IV. Experimental Verification

Experiments are performed, in order to verify the relationship between harvesting factor and non-dimensional rectified voltage $\tilde{V}_{rect}$ in the standard energy harvesting application, as given in Eq. (7); as well as the relationship between dissipation factor and non-dimensional resistance ρ in the resistive shunt damping application, as given in Eq. (11).

A. Standard energy harvesting

For standard energy harvesting, the experimental setup is shown in Fig. 7. One end of a commercial piezoelectric bimorph (QuickPack QP20W, Midé Technology) is fixed on a shaker (Mini Shaker Type 4810, Brüel & Kjær) to form a base-driven cantilever. In order to enhance the vibration at low frequency, a proof mass is mounted at the other end of the bimorph. It is measured that this piezoelectric cantilever

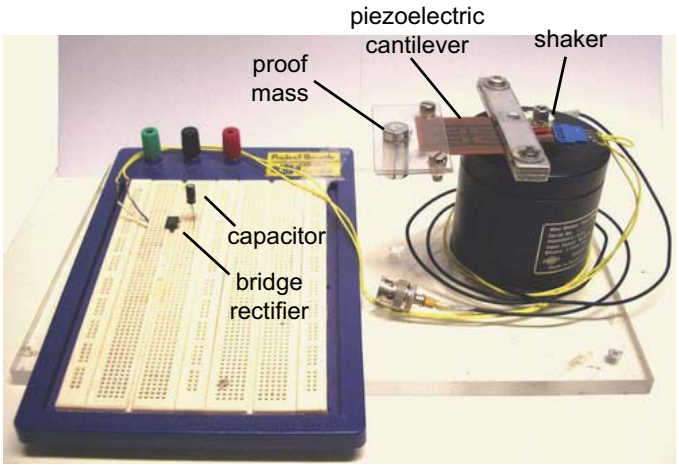

Fig. 7. Experimental setup for standard energy harvesting.

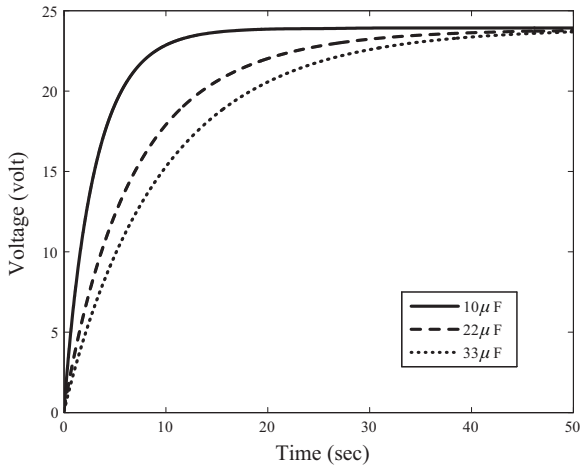

Fig. 8. Time histories of voltage with different storage capacitors.

has a natural frequency of 21.5Hz at open circuit and 20.6Hz at short circuit. Thus

$$k_{sys}^2 = \frac{\omega_{oc}^2 - \omega_{sc}^2}{\omega_{oc}^2}, \tag{19}$$

the coupling coefficient of this structure k_{sys}^2 is around 8.20%. The two layers of the bimorph are connected in series, and a capacitance of 42nF is measured. To harvest energy, the two electrodes are connected to the AC input port of a bridge rectifier, whose DC output port is connected to a capacitor for energy storage.

A 25Hz excitation signal is provided to the shaker. Its amplitude is adjusted until the open circuit voltage, i.e. V_{oc}, of the piezoelectric patch reaches 25V. To obtain the harvested energy per cycle, i.e. E_h in Eq. (1), with respect to different rectified voltage, the voltage rising across the storage capacitor is captured with a sampling frequency of 1kHz. Fig. 8 shows the voltage histories for charging three different capacitors, respectively. Their capacitance values are 10μF (measured 10.04μF), 22μF (measured 22.64μF) and 33μF (measured 30.94μF). It can be seen from the figure that, the smaller in value of storage capacitor, the quicker to be charged up. The obtained data is then processed in PC with Matlab. Assuming the mean voltage across the storage capacitor within an interval to be constant during charging, the harvesting power under this V_{rect} value can be obtained, because the energy input of the capacitor within such interval can be estimated according to the voltage change. However, there is a problem that the estimating interval should be chosen carefully. If it is too long, the constant voltage assumption would be invalid; on the contrary, if it is too short, the voltage across the capacitor can hardly change. We overcome this problem with an "adaptive interval algorithm". Generally, shorter interval for lower V_{rect} and longer one for higher V_{rect}, since the voltage changes more shapely at low V_{rect}.

To calculate the harvesting factor, there is still another challenge. Since the cantilever does not vibrate with constant displacement in the charging process, to estimate the loss factor, we need to know E_{max} in Eq. (1). This vibration energy is related to the maximum displacement in one vibration cycle. Therefore, an inductive displacement sensor (JCW-24SR, CNHF Co.) is used here to measure the displacement of the cantilever, so that we can adjust the estimation of E_{max} with the changing displacement.

Since the harvesting factor is also the loss factor in the standard energy harvesting, Fig. 9(a) shows the relation between the loss factor and non-dimensional rectified voltage in this application. According to Eq. (7), the solid curve shows the theoretical result with an ideal bridge rectifier. The three sorts of discrete marks are experimental results obtained from the corresponding voltages. Three of them are in good agreement, but all are lower than the solid theoretical curve. This difference may be due to the nonideal behavior of the diode bridge and nonideal sinusoidal current output from the piezoelectric patch[2]. To compensate this, a revisory factor considering the voltage drop across the rectifier is introduced, which is

$$\lambda = \frac{V_{rect} - 2V_{diode}}{V_{rect}}, \tag{20}$$

where V_{diode} is the voltage drop of a single diode. The V_{diode} is 0.5V for the bridge rectifier we used in this experiment. Multiplying Eq. (7) by λ yields the dash curve in Fig. 9(a). It is closer to the experimental results than the solid one.

B. Resistive shunt damping

For the experiment on resistive shunt damping, the mechanical part of the setup is the same as that for the standard energy harvesting. The difference is to replace the bridge rectifier and the storage capacitor with a resistor.

With the same excitation frequency, several chosen resistors at different values are connected to the piezoelectric patch one

[2]In our experiment, we found the lower the excitation frequency, the more deformation the open circuit voltage of this piezoelectric patch. In particular, for frequencies below 20Hz, the output can hardly be regarded as sinusoidal.

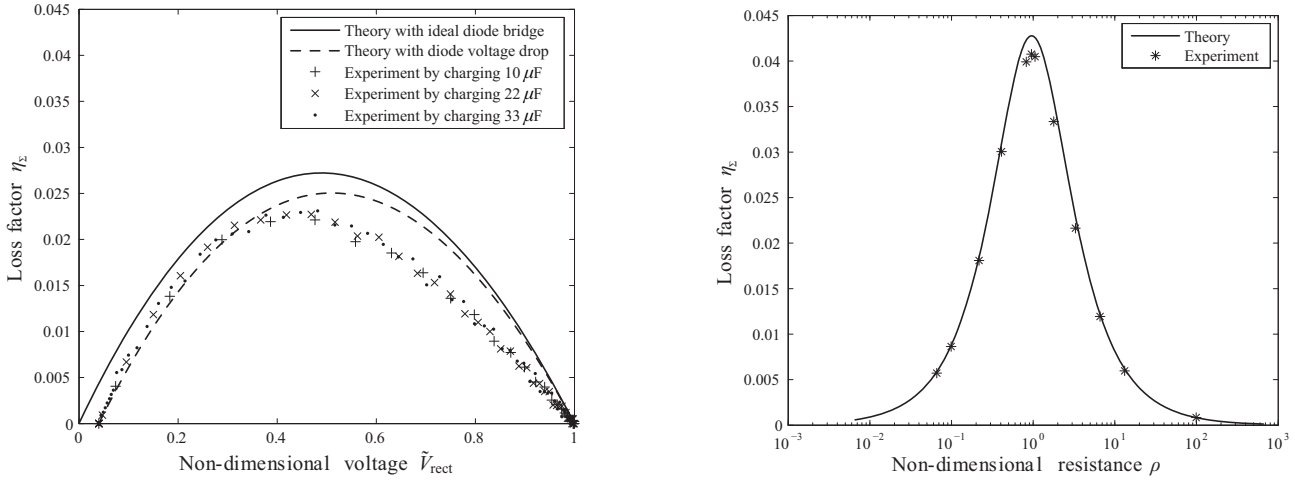

Fig. 9. Theoretical and experimental loss factors in two applications. (a) Standard energy harvesting. (b) Resistive shunt damping.

after another. For different shunt resistors, the displacement of the cantilever is adjusted to the same level according to the output of the displacement sensor, in order to have constant displacement excitation. With the RMS voltages across different resistors, we can calculate how much power is consumed by every single shunt resistor, and then the dissipation factor can be obtained.

As no energy is harvested in the application of resistive shunt damping, the dissipation factor here is also the loss factor. Fig. 9(b) shows the loss factor as a function the non-dimensional shunt resistance, both theoretically and experimentally. The two results show good agreement with each other.

As discussed above, even the energy flows in the two applications of standard energy harvesting and resistive shunt damping are different, they both extract energy from the vibrating mechanical structure, thus result in structural damping. Fig. 9(a) and (b) provide a comparison on the damping capabilities of these two applications at the condition of $k^2 = 8.20\%$. The results verify that the ratio of $(\eta_{\Sigma,max})_{SEH}$ to $(\eta_{\Sigma,max})_{RSD}$ is about 60% at low coupling conditions.

V. Conclusion

In this paper, we aimed to clarify the similarities and differences between the two functions of energy harvesting and energy dissipation in piezoelectric devices. Through theoretical analysis and experimental verification, these provide us with in-depth understanding on the energy harvesting and dissipation in piezoelectric devices. Two applications of standard energy harvesting and resistive shunt damping were studied as examples. Even for different objectives in utilization, the energy relations between these two applications were discussed and compared, in terms of damping capabilities. Experiments on these two applications verified the theoretical analysis. For the future research on energy harvesting technology, it is suggested that both functions of energy harvesting and dissipation could be considered simultaneously, so as to develop a more efficient and adaptive energy harvesting system.

Acknowledgments

The work described in this paper was supported by a grant from Innovation and Technology Commission of Hong Kong Special Administration Region, China (Project No. ITP/011/07AP). The authors would also like to thank Dr. Mingjie Guan for his constructive discussions and help in experiments.

References

[1] S. Beeby, M. Tudor, and N. White, "Energy harvesting vibration sources for microsystems applications," *Meas. Sci. Tech.*, vol. 17, no. 12, pp. R175–R195, Dec. 2006.

[2] G. Ottman, H. Hofmann, A. Bhatt, and G. Lesieutre, "Adaptive piezoelectric energy harvesting circuit for wireless remote power supply," *IEEE Trans. Power Elec.*, vol. 17, no. 5, pp. 669–676, 2002.

[3] A. Badel, D. Guyomar, E. Lefeuvre, and C. Richard, "Efficiency enhancement of a piezoelectric energy harvesting device in pulsed operation by synchronous charge inversion," *J. Intell. Mater. Syst. Struct.*, vol. 16, no. 10, pp. 889–901, 2005.

[4] S. R. Anton and H. A. Sodano, "A review of power harvesting using piezoelectric materials (2003-2006)," *Smart Mater. Struct.*, vol. 16, no. 3, pp. R1–R21, 2007.

[5] G. A. Lesieutre, G. K. Ottman, and H. F. Hofmann, "Damping as a result of piezoelectric energy harvesting," *J. Sound Vibr.*, vol. 269, pp. 991–1001, Jan. 2004.

[6] S. Moheimani, "A survey of recent innovations in vibration damping and control using shunted piezoelectric transducers," *IEEE Trans. Contr. Syst. Tech.*, vol. 11, no. 4, pp. 482–494, July 2003.

[7] C. M. Harris, *Shock and Vibration Handbook*. McGraw-Hill, 1996.

[8] C. W. de Silva, *Vibration and Shock Handbook*. CRC Press, 2005.

[9] D. J. Warkentin and N. W. Hagood, "Nonlinear piezoelectric shunting for structural damping," *Proc. SPIE conf. Smart Struct. Mater.*, vol. 3041, pp. 747–757, June 1997.

[10] D. Guyomar, A. Badel, E. Lefeuvre, and C. Richard, "Toward energy harvesting using active materials and conversion improvement by nonlinear processing," *IEEE Trans. Ultras. Ferro. Freq.*, vol. 52, no. 4, pp. 584–595, 2005.

[11] N. W. Hagood and A. von Flotow, "Damping of structural vibrations with piezoelectric materials and passive electrical networks," *J. Sound Vibr.*, vol. 146, pp. 243–268, Apr. 1991.